Polyhedron 30 (2011) 2421–2429

Contents lists available at ScienceDirect

Polyhedron

journal homepage: www.elsevier.com/locate/poly

ESR and pH-potentiometric study of the mixed–ligand complex formation in the copper(II)–4-fluorosalicylic acid–*N*,*N*-diethylnicotinamide system: Structure and spectral properties of [Cu(4-fluorosalicylate)$_2$(*N*,*N*-diethylnicotinamide)$_2$(H_2O)$_2$] complex

Terézia Szabó-Plánka [a], Ján Moncol [d], Eszter Tóth [c], Béla Gyurcsik [c], Nóra Veronika Nagy [b], Zuzana Vasková [d], Antal Rockenbauer [b], Dušan Valigura [d,*]

[a] Department of Physical Chemistry and Materials Sciences, University of Szeged, Aradi vértanúk tere 1, H-6720 Szeged, Hungary
[b] Chemical Research Center, Institute of Structural Chemistry, Hungarian Academy of Sciences, Pusztaszeri út 59-67, H-1025 Budapest, Hungary
[c] Department of Inorganic and Analytical Chemistry, University of Szeged, Dóm tér 7, Szeged H-6720, Hungary
[d] Department of Inorganic Chemistry, Slovak Technical University, Radlinskeho 9, 812 37 Bratislava, Slovakia

ARTICLE INFO

Article history:
Received 21 April 2011
Accepted 29 June 2011
Available online 12 July 2011

Keywords:
Copper(II) complexes
4-Fluorosalicylic acid
N,*N*-Diethylnicotinamide
Speciation
Electron spin resonance
pH-potentiometry
Crystal structure

ABSTRACT

EPR simulation method together with pH-potentiometry combined with UV–Vis spectrophotometry were used for the study of the ternary system 4-fuorosalicylic acid (H**A**)–*N*,*N*-diethylnicotinamide (**B**)–copper(II) in aqueous solution. The *N*,*N*-diethylnicotinamide ligand is a weak donor, its mixed–ligand complexes with 4-fluorosalicylate anions are more favoured. The number of coordinated *N*,*N*-diethylnicotinamide molecules increases with decreasing temperature: up to four ones were detected in the coordination sphere of copper(II) in frozen solutions. The formation of [CuH_{-1}**AB**$_2$] and [CuH_{-1}**A**] was detected by all methods at neutral pH. At lower pH values, [Cu**A**$_2$**B**$_2$] and [Cu**B**] become dominant, and this fact is in good agreement with [Cu**A**$_2$**B**$_2$(H_2O)$_2$] crystals obtained from similar solutions. The structural unit of the [Cu**A**$_2$**B**$_2$(H_2O)$_2$] complex consists of a copper(II) ion, which is monodentately coordinated by a pair of 4-fluorosalicylate anions and by a pair of *N*,*N*-diethylnicotinamide in *trans* positions in the basal plane, and by two water molecules in the axial positions of a tetragonal bipyramid.

1. Introduction

The great attention of many research groups dealing with the role played by therapeutically active substances in organisms has been in the latest decades focused to the metal complex formation [1–8]. The most mentioned biological characteristics of the *N*,*N*-diethylnicotinamide (abbreviated as den) is its "breathing stimulant" activity [9] and it still is in use nowadays [10]. Its possible interactions with different biometals in living systems and proven biological activity of some complexes [11–15] are the reasons for the substantial interest of bioinorganic chemists in these complexes. This could be documented by about seventy metal complexes with known structure, and the copper(II) complexes with den ligands are more than half of all ones. The den ligand is in complexes usually bonded monodentately *via* the pyridine nitrogen donor atom, and rarely a bridging *N*,*O* mode could be found too. There are three different Cu(II):den stoichiometries observed in the group of carboxylatocopper(II) complexes. In few cases, 2:1 stoichiometry and bridging mode of den bonding has been found in the polymeric [Cu_2(RCOO)$_4$(den)]$_n$ complexes built up of dimeric Cu_2(RCOO)$_4$ molecules and den ligands [16,17]. Another rare Cu(II):den stoichiometry is 1:1, that could be found in paddle–wheel complexes [11,12,18,19] of the type [Cu_2(RCOO)$_4$(den)$_2$] and in polymeric [Cu(RCOO)$_2$(den)(H_2O)] complexes that were just recently published [20,21]. The most frequent 1:2 stoichiometry with unidentate den ligands can be found in monomeric complexes of general formula Cu(RCOO)$_2$(den)$_2$(H_2O)$_x$, where x = 0 [22,23], x = 2 [17,24–29] or x = 4 [30]. Within the structural study of the group [Cu(x-Me(O)sal)$_2$(den)$_2$(H_2O)$_2$] (where x-Me(O)-sal = x-methyl- or x-methoxy-salicylate, x = 3, 4 or 5), the conformational polymorphism with its consequence in supramolecular isomerism has been found [29] for the pair of [Cu(3-Mesal)$_2$(den)$_2$(H_2O)$_2$] complexes.

Salicylic acid itself [31] and its derivatives [32–39] have been studied for their therapeutic performance that have led to the thorough investigation of their properties in the presence of copper(II) because of its ability to act in a synergistic manner with the salicylic acid derivatives [40–44], the mechanism of which is not yet fully understood. Our recent attention focused on the various

* Corresponding author.
E-mail address: dusan.valigura@stuba.sk (D. Valigura).

0277-5387/$ - see front matter © 2011 Elsevier Ltd. All rights reserved.
doi:10.1016/j.poly.2011.06.030

isomers of fluorosalicylic acids and their complexes in solid state and in solutions [45–48] is in the present paper oriented toward the system containing copper(II) ions in the presence of 4-fluorosalicylic (4F-sal) acid and *N*,*N*-diethylnicotinamide.

2. Experimental

2.1. Materials

The ligands 4-fluorosalicylic acid and *N*,*N*-diethylnicotinamide were of analytical grade, and were purchased from Aldrich Chemical Co. They are symbolized by H**A** and **B** in their neutral forms, respectively, when giving the composition of various complexes. Doubly deionized water and freshly distilled methanol were used as solvents. Copper(II) perchlorate (Fluka) solutions were standardized complexometrically. The pH-metric titrations were performed with NaOH (Aldrich) standard solution. To ensure acidic starting conditions, $HClO_4$ (Aldrich) was added to the solutions before titration. Other reagents were of analytical grade, supplied by Aldrich or Sigma, and were used as received.

2.2. Preparation of [Cu(4-fluorosalicylate)$_2$(*N*,*N*-diethylnicotinamide)$_2$(H_2O)$_2$] complex

The title compound was prepared by mixing an aqueous solution of copper(II) acetate (0.32 mmol) with an aqueous solution (about 80 mL) containing mixture of 4-fluorosalicylic acid (0.64 mmol) with *N*,*N*-diethylnicotinamide (0.64 mmol). The reaction mixture was stirred until the reaction finished and the color of the product remained unchanged. The light blue microcrystalline product which precipitated was filtered off and mother liquor was left to crystallize at ambient temperature. The blue crystals suitable for X-ray structure determination were separated after several days and dried at ambient temperature.

2.3. pH-metric measurements

The protonation and coordination equilibria were investigated by potentiometric titrations in aqueous solution (I = 0.1 M $NaClO_4$, and T = 298.0 ± 0.1 K) under argon atmosphere, using an automatic titration set including a PC controlled Dosimat 665 (Metrohm) autoburette and an Orion 710A precision digital pH-meter. The Metrohm semimicro combined pH glass electrode (125 mm) was calibrated [49] *via* the modified Nernst Eq. (1):

$$E = E_0 + K \cdot \log[H^+] + J_H \cdot [H^+] + \frac{J_{OH} \cdot K_w}{[H^+]} \quad (1)$$

where J_H and J_{OH} are fitting parameters in acidic and alkaline media for the correction of experimental errors, mainly due to the liquid junction and to the alkaline and acidic errors of the glass electrode; $K_w = 10^{-13.75}$ M^2 is the autoprotolysis constant of water [50]. The parameters were calculated by the non-linear least squares method. The complex formation was characterized by the following general equilibrium process (2):

$$pCu + qH + rA + sB \overset{\beta_{Cu_pH_qA_rB_s}}{\rightleftharpoons} Cu_pH_qA_rB_s$$
$$\beta_{Cu_pH_qA_rB_s} = \frac{[Cu_pH_qA_rB_s]}{[Cu]^p[H]^q[A]^r[B]^s} \quad (2)$$

where Cu denotes the metal ion, while **A** and **B** the non-protonated ligands (**A** = 4-fluorosalicylate anion and **B** = *N*,*N*-diethylnicotinamide molecule). Here and in the figures the charges are omitted for simplicity, but they can easily be calculated taking into account the compositions and charges of the fully protonated ligands. The corresponding formation constants ($\beta_{Cu_pH_qA_rB_s} \equiv \beta_{pqrs}$) were calculated using the PSEQUAD computer program [51].

The protonation constant of the **B** ligand was determined from 3 independent titrations (80–90 data points per titration), the protonation constant of **A** ligand was previously determined [48]. The complex formation constants of the copper(II)–**B** binary system and of the copper(II)–H**A**–**B** ternary system were evaluated from 4 to 6 independent titrations (50–90 data points per titration). The metal-to-ligand ratios varied between 1:1 and 1:100 in the copper(II)–**B** system; 1:2:2 and 1:2:4 in the copper(II)–H**A**–**B** system, and the ligand concentrations between 8.9×10^{-4}–1.8×10^{-3} M for H**A** and 4.5×10^{-4}–1.0×10^{-1} M for **B**.

2.4. UV–Vis spectroscopic measurements

UV–Vis absorption spectra in aqueous solutions were recorded by means of Ocean Optics PC2000 plug in fiber optic spectrophotometer, in the wavelength interval from 350 to 800 nm, 1 cm optical pathlength, and by a Hewlett Packard 8452 diode array spectrophotometer in a quartz cell of 4 cm optical pathlength.

2.5. X-ray crystallography

Data collection and cell refinement were carried out using a κ-axis diffractometers Bruker Kappa APEXII CCD [52] at 150 K with graphite monochromated Mo Kα radiation. The diffraction intensities were corrected for Lorentz and polarization factors. The structure was solved by direct methods using SIR-97 [53] and refined by the full-matrix least-squares procedure with SHELXL-97 [54]. The multi-scan absorption correction was applied the program SADABS [55]. Geometrical analyses were performed with SHELXL-97. The structures were drawn with XP in SHELXTL [54] and PLATON [56]. The crystal data, conditions of data collection and refinement are reported in Table 1.

2.6. ESR measurements

The total (analytical) copper(II) concentration, T_{Cu} was 1 mM in all cases. For the Cu(II)–H**A** system, the total ligand concentration T_A = 2 mM was applied, while for the Cu(II)–**B** system, T_B was 2, 5 or 25 mM. For the Cu(II)–H**A**–**B** system, T_A was 2 mM and T_B was

Table 1
Crystallographic data for **1** complex.

	1
Code	RS36ml1
Chemical formula	$C_{34}H_{40}CuF_2N_4O_{10}$
M_r	766.24
Cell setting, space group	triclinic, $P\bar{1}$
T (K)	150(2)
a (Å)	7.5360(5)
b (Å)	8.2930(4)
c (Å)	14.4060(12)
α (°)	85.312(6)
β (°)	81.244(7)
γ (°)	76.513(6)
V (Å^3)	864.39(10)
Z	1
Radiation type	Mo Kα
μ (mm^{-1})	0.706
Crystal size (mm)	0.497 × 0.216 × 0.176
Diffractometer	Bruker Kappa APEXII CCD
Absorption correction	SADABS
T_{min}, T_{max}	0.719, 0.883
S	1.084
$R_1[F^2 > 2\sigma(F^2)]$, $wR_2(F^2)$	0.0360, 0.0781
Data/restrains/parameters	3548/0/235
$\Delta\rho_{max}$, $\Delta\rho_{min}$ (e Å^{-3})	0.186, −0.164

2, 5 or 25 mM. The pH was adjusted with NaOH (0.2 M) to a value between 4.60 and 4.67, to an accuracy of 0.01 pH unit, measured with a Radiometer PHN 240 pH-meter equipped with a Metrohm LL combined microelectrode, which was calibrated with IUPAC Standard Buffers (Radiometer). The ESR spectra were recorded at 298 K using an X-band Bruker EleXsys E500 instrument. Before the measurements, the signal of the capillary tube filled with distilled water was recorded as background.

Samples of 0.100 cm^3 volume were taken from the solutions at 298 K, 0.010 cm^3 methanol was added to each, and after mixing they were frozen in liquid nitrogen. Then the ESR spectra were recorded at 77 K with the same spectrometer as above.

2.7. Evaluation of ESR spectra

Analysis of the isotropic spectra recorded at 298 K was preceded by the elimination of the background signal. Then the spectra were evaluated by the EPR program [57], which allows to take in consideration one to four component curves. The ESR spectra of the various species were described by the parameters g_0, the copper hyperfine coupling constant A_0, the nitrogen superhyperfine coupling constant a_{N0} and the relaxation parameters α, β and γ relating to the line widths of the copper hyperfine multiplet as $W_{M_I} = \alpha + \beta M_I + \gamma M_I^2$ (M_I is the magnetic quantum number of copper nuclei). Since a natural mixture of copper isotopes was used, the spectra were calculated as the sum of the curves of molecules containing isotope ^{63}Cu or ^{65}Cu weighted by their natural abundances. The hyperfine coupling constants and the relaxation parameters given in the Tables refer to the ^{63}Cu isotope. The coupling constants and the relaxation parameters are given in gauss (G) units throughout the paper 1 G = 10^{-4} T.

The quality of fit for the *j*th spectrum was characterized by the noise-corrected regression parameter R_j computed from the average square deviation between the respective experimental and calculated curves. The noise was deduced from the quadratic error of the fit to obtain $R_j = 1$ for perfect fit.

For the anisotropic ESR spectra, the EPR program allows the description of the experimental spectra as the superposition of one to three component curves. The spectral fits (characterized by the noise-corrected regression parameter R_j, see above) achieved with the assumption of either axial or rhombic g-, hyperfine, superhyperfine, and quadrupole coupling tensors were compared to gain information about the symmetry of the coordination polyhedron in various species. Anisotropy of the relaxation parameters α, β and γ was also taken into consideration. In some cases, a rhombic zero-field splitting was also considered. Calculated spectra were composed of the curves of complexes containing isotope ^{63}Cu or ^{65}Cu as for the isotropic spectra.

3. Results and discussion

3.1. Solution speciation in the copper(II)–H**A**–**B** system

Under the conditions described in the experimental part, 4-fluorosalicylic acid (H**A**) undergoes one deprotonation process up to pH 11, which is related to the carboxylic group with a pK_a of 2.76 [48]. Similarly, only one protonation process of the *N*,*N*-diethylnicotinamide (**B**) was observed. The proton complex was defined as $[HL]^+$, its pK_a = 3.34(1) is very close to that determined for nicotinamide (pK_a = 3.3 [58]; pK_a = 3.6 ± 0.2 [59]; pK_a = 3.42; [60]; pK_a = 3.42 [61]).

Since there were no literature data under the present conditions for the copper(II)–**B** system, we first investigated the binary complexes. The low pK_a of **B**, as expected, allows for the formation of parent complexes with low stability, and therefore, rather poor conditions for their pH-metric detection. In order to promote complexation, we varied the metal-to-ligand ratio from 1:1 to 1:100. The buffering effect of the large quantity of the ligand at high ligand excess, however, prevented to detect significant pH effect attributed to the complex formation. Finally, in the acidic pH range the complex $[Cu\mathbf{B}]^{2+}$ could only be detected by pH-metry (Table 2). On the other hand, the UV–Vis absorption maxima of the solutions with increasing ligand excess continuously shifted from ~800 nm (Cu:**B** = 1:2) to ~706 nm (Cu:**B** = 1:100) at pH ~4.5. This clearly shows that parent complexes with more ligand molecules were formed in the solutions, too. Similarly, stepwise formation of the parent complexes was detected by the ESR measurements under high ligand excess (see Section 3.3). The formation of these, however, occurred in the pH range where **B** was in non-protonated form, therefore, it did not cause a significant pH effect, and hence, the stability constant for these species could not be determined accurately by pH-potentiometry.

The low stability of these complexes was not able to prevent the hydrolytic processes of copper(II) around pH 6.5. It was also observed that the deprotonation step(s) – resulting in the formation of $Cu(OH)_2$ precipitate and/or $[CuH_{-1}\mathbf{B}]^+$ and $CuH_{-2}\mathbf{B}$ complexes – were shifted to higher pH (by about 0.5 unit) at 100-fold ligand excess, indicating that more ligand molecules around the metal ion can hinder the hydrolytic processes.

The ternary complex formation in aqueous solution was investigated by pH-potentiometric titrations carried out under similar conditions than the crystallization experiments (see later), in 1:2:2 or 1:2:4 copper(II):H**A**:**B** systems. The stability constants of the species yielding the best fit with the experimental titration curves are collected in Table 2. The species distribution diagram of the latter system (Fig. 1) shows that the ternary complexes dominate over the binary ones in the whole pH range. The first complexes were $[Cu\mathbf{B}]^{2+}$ and $[Cu\mathbf{A}_2\mathbf{B}_2]$ with concentration maxima at pH 4.0 and 4.3, respectively. The latter is most probably the species that crystallized from the solution (see Section 3.2). Under these conditions, a substantial amount of the aqua complex is still present, but significantly less than in the Cu:H**A** 1:2 or Cu:**B** 1:4 systems, indicating the enhanced formation of the ternary complexes. The shift of the absorption maximum (λ_{max} ~ 750 nm) compared to the binary systems (λ_{max} ~ 765 nm for Cu:H**A** 1:2, and λ_{max} ~ 798 nm for Cu:**B** 1:4) suggests an increased ligand field around the metal ion, in accordance with the coordination of two carboxylate oxygens of molecules **A**, and two pyridyl nitrogens from ligands **B**, similar to the coordination mode in the crystals.

The next deprotonation step results in a chelate-type complex by the coordination of the phenolate and carboxylate oxygens of one of the 4-fluorosalicylate ligands. The development of the band at ~390 nm in the UV–Vis absorption spectra corresponding to the phenolate–copper(II) charge transfer (CT) [45], and the ESR spectra also support this. Simultaneously, the rearrangement of the coordination sphere occurs: one of the **B** or the second **A** ligand must be

Table 2
The stability constants of the species included in the characterization of the copper(II)–**A**–**B** system (4-fluorosalicylic acid = H**A** and *N*,*N*-diethylnicotinamide = **B**).

Species	log β
HA	2.76[a]
$[HB]^+$	3.34(1)
$CuH_{-1}A$	−2.59[a]
$[CuH_{-2}A_2]^{2-}$	−7.70[a]
$[Cu_2H_{-3}A_2]^-$	−10.37[a]
$[CuB]^{2+}$	2.47(4)
CuA_2B_2	11.91(4)
$CuH_{-1}AB_2$	3.79(1)
$[CuH_{-2}AB]^-$	−7.55(2)

[a] From Ref. [48]. The uncertainty of the constants is shown in parentheses.

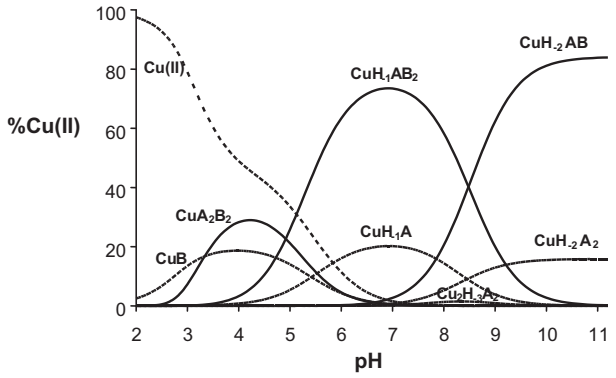

Fig. 1. The species distribution diagram for the Cu:**A**:**B** = 1:2:4 system calculated on the basis of the stability constants depicted in Table 1. The ternary species are represented by solid lines while other species with dashed lines. $c_{Cu(II)} = 5.0 \times 10^{-4}$ M; I = 0.1 M, $NaClO_4$; T = 298 K.

pulled out from the equatorial coordination. It is worth to note that the deprotonation in the ternary system occurred at lower pH than in the Cu:**A** binary system, and so the overlapping equilibria make the assignment of the macroscopic processes to the individual deprotonation steps ambiguous. The intensity of the above-mentioned UV-band suggests somewhat higher amount of the deprotonated complexes than the macroscopic species distribution does. The spectral data suggest that the composition of this complex is [CuH$_{-1}$**AB**$_2$] rather than [Cu(H$_{-1}$**A**)**AB**]$^-$ (see later). The formation of neutral ternary complexes ([Cu**A**$_2$**B**$_2$] and [CuH$_{-1}$**AB**$_2$]) may enhance the passage of **B** across the hydrophobic cell membranes by passive diffusion, while the passage for the charged molecules (like H**B**$^+$ in acidic media) is expected to be slow in the absence of a carrier [62].

At pH ~7.0, a new deprotonation process started that could be best fitted with the composition of [CuH$_{-2}$**AB**]$^-$, similarly to the ternary system copper(II)–3-pyridylmethanol–5-fluorosalicylic acid [63]. In this complex, one of the **B** ligands is probably replaced by a deprotonated water molecule, resulting in the {COO$^-$, phenolate-O$^-$, pyridyl-N, OH$^-$} coordination around the copper(II) ion.

The coordination modes for two of the mixed–ligand complexes could be characterized in more detail: [Cu**A**$_2$**B**$_2$] was obtained also in the crystalline state, and it was investigated by X-ray diffraction and UV–Vis and IR spectroscopy, while ESR spectroscopic data offered information on the structure of [CuH$_{-1}$**AB**$_2$] in solution. Furthermore, the ESR spectroscopic studies revealed some features of the copper(II)–**B** binary equilibrium system, too.

Table 3
Selected geometric parameters (Å, °).

	1
Cu1–N1	2.006(2)
Cu1–O1	1.984(2)
Cu1–O1W	2.422(2)
O1–Cu1–N1	90.07(7)
O1–Cu1–O1W	92.65(7)
N1–Cu–O1W	92.01(7)
O1W···O2	2.723(3)
H1W···O2	1.92
O1W–H1W–O2	160
O1W···O4^{ii}	2.789(3)
H2W···O4^{ii}	1.97
O1W–H2W–O4^{ii}	165
O3···O2	2.536(3)
H3O···O2	1.79
O3–H3O···O2	146

Symmetry codes: (i) $-x+1, -y+1, -z+1$; (ii) $-x+2, -y, -z+1$.

3.2. Structure and spectral properties of [Cu**A**$_2$**B**$_2$(H$_2$O)$_2$]

The principal structural features of [Cu**A**$_2$**B**$_2$(H$_2$O)$_2$] (**1**) are illustrated in Fig. 2. Selected bond lengths and angles as well as structural parameters of hydrogen bonds of **1** are shown in Table 3. The coordination environment of the copper atom is elongated tetragonal bipyramidal. The tetragonal plane is built up by a pair of unidentate **A**$^-$ anions using carboxylate oxygen atoms [Cu1–O1 = 1.984(2) Å] and by a pair of neutral **B** molecules using pyridine ring nitrogen atoms [Cu1–N1 = 2.006(2) Å] in *trans* positions. The two axial positions of tetragonal bipyramid are occupied by two coordinated water molecules [Cu1–O1W = 2.422(2) Å], thus T parameter [64] is 0.82. Intramolecular hydrogen bonds involving an axial coordinated water molecule and uncoordinated carboxylate oxygen atoms [O1W–H1W···O2, with O1W···O2 distance 2.723(3) Å], stabilize the molecular structure of **1**. The hydroxyl groups of **A**$^-$ anions are connected into intramolecular hydrogen bonds [O3–H3O···O2, with O3···O2 distance 2.536(3) Å] in six-membered intramolecular rings $S(6)$ [65], where the acceptors of hydrogen bonds are also uncoordinated carboxylate oxygen atoms of **A**$^-$ anions. Similar coordination environments around the copper atoms have been observed in the crystal structures of some methyl- and methoxysalicylatocopper(II) complexes [29,30] as well as other [Cu(RCOO)$_2$(den)$_2$(H$_2$O)$_2$] complexes [17,20,24–28]. The orientation of the pyridine rings in relation to the equatorial planes of the coordination polyhedra, and the value of the dihedral

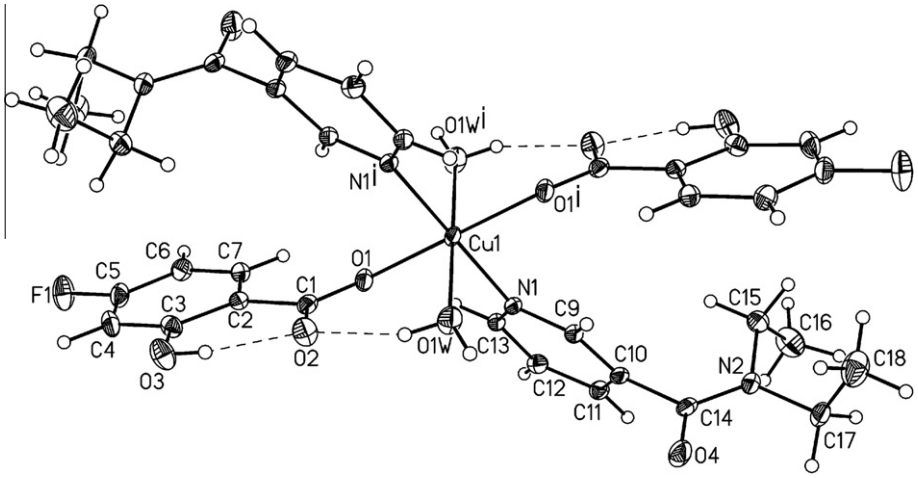

Fig. 2. Perspective view of **1** complex, with the atom numbering scheme. Thermal ellipsoids are drawn at the 30% probability level.

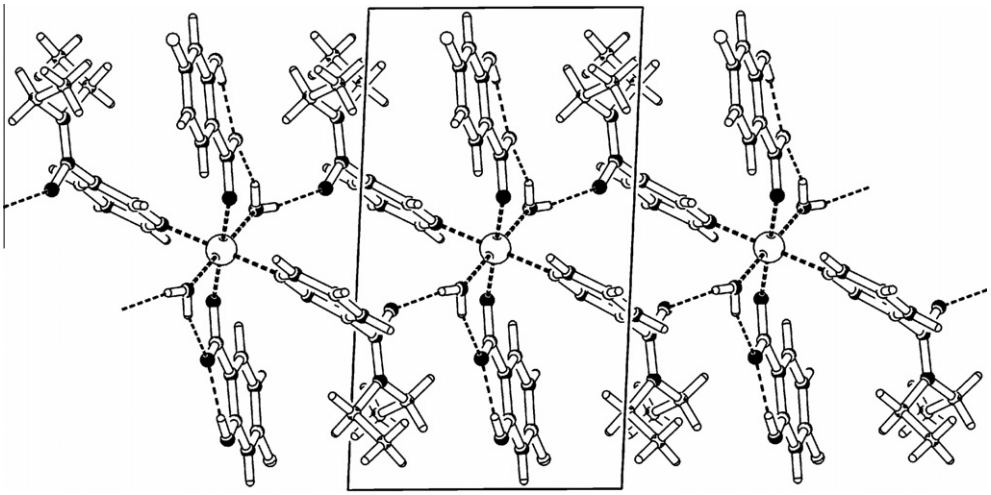

Fig. 3. Supramolecular chain from molecules of **1**, connecting through O–H···O hydrogen bonds.

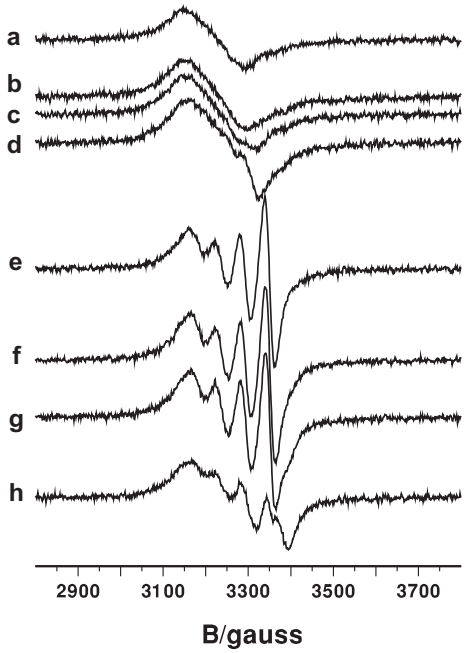

Fig. 4. Isotropic ESR spectra in aqueous solution at 298 K; (a) $CuCl_2$ solution, pH 3.8; (b)–(e) binary systems at T_{Cu} = 1 mM: (b) T_B = 2 mM, pH 4.66; (c) T_B = 5 mM, pH 4.67; (d) T_B = 25 mM, pH 4.65; (e) T_A = 2 mM, pH 4.60; (f)–(h) ternary systems at T_{Cu} = 1 mM and T_A = 2 mM: (f) T_B = 2 mM, pH 4.67; (c) T_B = 5 mM, pH 4.66; (d) T_B = 25 mM, pH 4.67.

angle [38.2°] between the pyridine ring plane and the equatorial plane of the coordination polyhedron N1–O1–Cu–O1^{i}–N^{i} of complex **1** are very similar to those observed in the crystal structures of polymorph-II of [Cu(3-Mesal)$_2$(den)$_2$(H$_2$O)$_2$] (3-Mesal = 3-methylsalicylate anion) [29] and complex [Cu(4-MeOsal)$_2$(den)$_2$(H$_2$O)$_2$] (4-MeOsal = 4-methoxylsalicylate anion) [29]. All complexes show similar orientations of carboxamide groups, thus the C9–C10–C14–O4 torsion angles have similar values: 64.3° for **1**, 52.0° for [Cu(3-Mesal)$_2$(den)$_2$(H$_2$O)$_2$] [29], and 63.3° for [Cu(4-MeOsal)$_2$(den)$_2$(H$_2$O)$_2$] [29].

The molecules of **1** are joined by intermolecular hydrogen bonds [O1W–H2W···O4^{ii} [Symmetry code: (ii) $-x+2$, $-y$, $-z+1$), with O1W···O4^{ii} distance of 2.789(3) Å], between the hydrogen atoms of the coordinated water molecules and the amide oxygen atoms of **B** ligands of adjacent complexes molecules through $R_2^2(16)$ rings [65]. The $R_2^2(16)$ rings [65] form supramolecular chains in direction [1 $\bar{1}$ 0] (Fig. 3). The supramolecular chains are connected through π–π stacking interactions [66] between two pyridine aromatic rings of **B** ligands of two neighboring complex [$-x+1$, $-y$, $-z+1$]. The plane–plane and centroid–centroid distances of π–π stacking interactions are 3.38 and 3.47 Å, respectively.

In the IR spectrum of the complex, the bands assigned to $\nu_{as}(COO^-)$ and $\nu_s(COO^-)$ are at 1610 and 1369 cm^{-1}, respectively. The value of $\Delta\nu$ ($\Delta\nu = \nu_{as} - \nu_s$ = 241 cm^{-1}) is greater than $\Delta\nu$ for the ionic form of the 4-fluorosalicylate salt (158 cm^{-1}), and corresponds to an unidentate mode of coordination [67]. The band at 3494 cm^{-1} corresponds to the OH vibration and confirms the presence of water molecules in the compound.

The solid state electronic spectrum of the complex exhibits a broad asymmetrical absorption band attributed to $d \leftarrow d$ transitions with maximum positioned at about 631 nm, typical of tetragonal–bipyramidal copper(II) [68].

3.3. ESR spectra in liquid solution at 298 K

The isotropic ESR spectra recorded at pH ~4.6 are shown in Fig. 4. The curves of the Cu(II)–**B** system at a 2- or 5-fold excess of ligand are very similar to the spectrum of the $CuCl_2$ solution {containing the aqua complex [Cu(aqua)]$^{2+}$}. Evaluating with one component spectrum, the parameters slightly differed from those of the aqua complex, however, if two or three components were considered, the ESR parameters became uncertain. Most probably, the major species is the aqua complex in these solutions, too, and the minor species also have broad, unresolved spectra with similar g and A that makes the decomposition of experimental curves uncertain. At 25-fold excess of **B** (Fig. 4d), two component spectra could be identified. Comparing their parameters (Table 4) to the data of the 3-pyridylmethanol complexes [47], the major one can be assigned to [Cu**B**]$^{2+}$, while the minor one to [Cu**B**$_2$]$^{2+}$. In contrast to the Cu(II)–3-pyridylmethanol system, the complexes [Cu**B**$_3$]$^{2+}$ and [Cu**B**$_4$]$^{2+}$ could not be shown at all, also indicating lower complexing ability of B, which can be explained by much lower basicity of its pyridyl nitrogen.

In the Cu(II)–H**A** system at pH 4.61 (Fig. 4e), the formation of two minor species{[Cu(aqua)]$^{2+}$ and [Cu**A**]$^{+}$} and a major complex {[CuH$_{-1}$**A**]} can be expected [48]. Accordingly, the experimental curve was decomposed into three component spectra. The param-

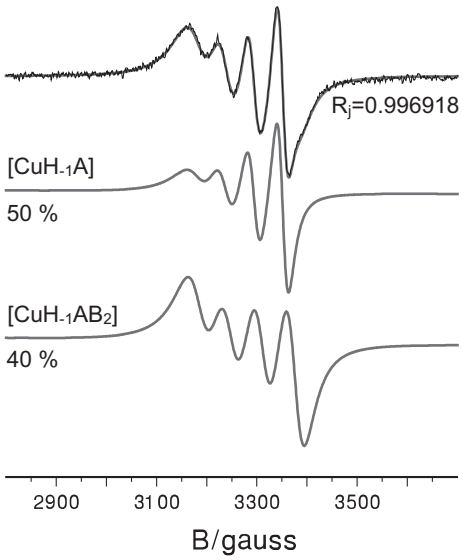

Fig. 5. Experimental curve (black line) taken in aqueous solution at 298 K, at T_{Cu} = 1 mM, T_A = 2 mM and T_B = 5 mM analytical concentrations, together with the curve calculated as a four-component spectrum (gray line). Its major components are shown below (gray line).

eters for the major one (Table 4) are in satisfactory agreement with the data for [CuH$_{-1}$**A**], obtained by the two-dimensional evaluation method in 50 v/v% methanol/water solvent mixture [48].

For the Cu(II)–H**A**–**B** system, the spectra (Fig. 4f and g) are reminiscent of the former one, however, a fourth, new component is also necessary for the good spectral fit (Fig. 5). The weight of this component curve (*i.e.* the concentration of the corresponding complex in the solution) increases in parallel with the increasing amount of **B**, while the contribution of [CuH$_{-1}$**A**] decreases (Table 4). At high excess of **B**, the new species becomes predominant (Table 4 and Fig. 4h). In accordance with the pH potentiometric findings, probably it is the mixed–ligand complex [CuH$_{-1}$**AB**$_2$]. Compared to [CuH$_{-1}$**A**], its lower g_0 and higher A_0 reflect on a stronger ligand field, which can be attributed to the equatorial coordination of the two **B** ligands through their pyridyl nitrogens. The line-broadening (Fig. 5) can be explained by a faster ligand exchange allowed by the monodentate coordination of molecules **B**. A similar phenomenon occurs in the Cu(II)–3-pyridylmethanol system [47], too.

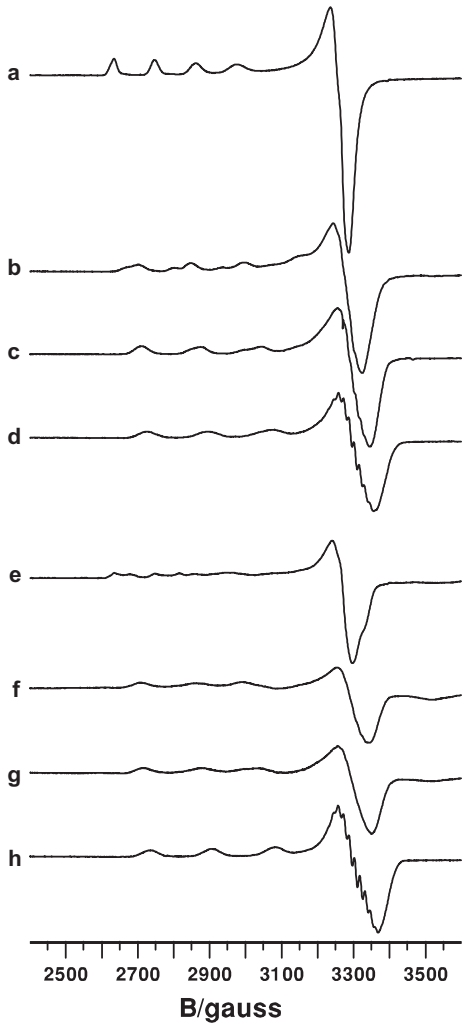

Fig. 6. Anisotropic ESR spectra in frozen 9 v/v% methanol/water at 77 K; (a) $CuCl_2$ solution, pH 3.8; (b)–(e) binary systems at T_{Cu} = 1 mM: (b) T_B = 2 mM, pH 4.66; (c) T_B = 5 mM, pH 4.67; (d) T_B = 25 mM, pH 4.65; (e) T_A = 2 mM, pH 4.60; (f)–(h) ternary systems at T_{Cu} = 1 and T_A = 2 mM: (f) T_B = 2 mM, pH 4.67; (c) T_B = 5 mM, pH 4.66; (d) T_B = 25 mM, pH 4.67.

The concentration data in Table 4 suggest that the binary complex [CuH$_{-1}$**A**] is more favoured in the ternary system than

Table 4
Isotropic ESR parameters[a] for the various complexes formed in the binary and ternary systems in aqueous solution at 298 K.

T_{Cu} (mM)	T_A (mM)	T_B (mM)	pH	g_0	A_0 (G)	α (G)	β (G)	γ (G)	Species	W (%)
1	0	0	3.80	2.191	30.7	50.0	−2.1	0.0	$[Cu(aqua)]^{2+}$	100
1	0	25	4.65	2.177	42.0	48.2	−1.4	1.7	$[Cu\mathbf{B}]^{2+}$	81
				2.150	51.0	36.0	−14.8	16.9	$[Cu\mathbf{B}_2]^{2+}$	19
1	2	0	4.61	f[b]	f	f	f	f	$[Cu(aqua)]^{2+}$	11
				f	f	f	f	f	$[Cu\mathbf{A}]^{+}$	3
				2.159	54.6	30.7	−7.3	0.6	[CuH$_{-1}$**A**]	86
1	2	2	4.67	f	f	f	f	f	$[Cu(aqua)]^{2+}$	9
				f	f	f	f	f	$[Cu\mathbf{A}]^{+}$	3
				2.160	55.1	29.9	−9.7	1.8	[CuH$_{-1}$**A**]	58
				2.151	60.6	38.9	−1.1	−0.4	[CuH$_{-1}$**AB**$_2$]	30
1	2	5	4.66	f	f	f	f	f	$[Cu(aqua)]^{2+}$	8
				f	f	f	f	f	$[Cu\mathbf{A}]^{+}$	2
				2.160	55.0	29.8	−9.5	1.9	[CuH$_{-1}$**A**]	50
				2.151	61.7	40.7	−4.0	0.0	[CuH$_{-1}$**AB**$_2$]	40
1	2	25	4.67	f	f	f	f	f	$[Cu(aqua)]^{2+}$	2
				2.153	59.7	44.8	−2.8	1.1	[CuH$_{-1}$**AB**$_2$]	98

[a] The estimated error for g_0 is 0.001, while for A_0 and the relaxation parameters it falls between 0.1 and 1.0 G.
[b] 'f' means that the respective parameter was fixed in the course of parameter fitting; for $[Cu(aqua)]^{2+}$, the values obtained from the analysis of the spectrum of the $CuCl_2$ solution, while for $[Cu\mathbf{A}]^{+}$, literature data from Ref. [47] were used.

Table 5
Anisotropic ESR parameters[a] for the various complexes formed in the binary and ternary systems in 9 v/v% methanol/water solution at 77 K.

T_{Cu} (mM)	T_A (mM)	T_B (mM)	pH	g_{xx}	g_{yy}	g_{zz}	g_0[b]	A_{xx} (G)	A_{yy} (G)	A_{zz} (G)	A_0 (G)[b]	$a_{N\perp}$ (G)[c]	D (G)	E (G)	Complex	W (%)
1	0	0	3.80	2.081	2.081	2.424	2.195	2.0	2.0	111.9	38.6				$[Cu(aqua)]^{2+}$	100
1	0	2	4.66	2.070	2.070	2.371	2.170	1.1	1.1	126.0	42.7	1.1			$[CuB]^{2+}$	42
				2.063	2.063	2.326	2.151	1.8	1.8	143.0	48.9	2.0			$[CuB_2]^{2+}$	58
1	0	5	4.67	2.055	2.055	2.319	2.143	1.3	1.3	141.1	47.9	0.0			$[CuB_2]^{2+}$	55
				2.064	2.064	2.294	2.141	14.3	14.3	166.5	65.0	7.6			$[CuB_3]^{2+}$	45
1	0	25	4.65	2.057	2.057	2.280	2.131	5.1	5.1	167.7	59.3	14.7			$[CuB_4]^{2+}$	100
1	2	0	4.01	2.081	2.081	2.423	2.195	1.6	1.6	109.4	37.5				$[Cu(aqua)]^{2+}$	43
				2.066	2.066	2.365	2.166	11.3	11.3	130.0	50.9				$[CuH_{-1}A]$	40
				2.290	2.081	2.436	2.269						537	−1	Dimer 1	17
1	2	2	4.67	2.061	2.061	2.314	2.145	15.6	15.6	147.9	59.7	13.1			$[CuH_{-1}AB_2]$	60
				2.230	2.059	2.369	2.219						517	−17	Dimer 2	40
1	2	5	4.66	2.060	2.060	2.300	2.140	13.3	13.3	159.6	62.1	12.4			$[CuH_{-1}AB_2]$	70
				2.270	2.065	2.371	2.235						525	−17	Dimer 2	30
1	2	25	4.67	2.054	2.054	2.273	2.127	6.0	6.0	169.6	60.5	14.4			$[CuB_4]^{2+}$	100

[a] The estimated error for g is 0.001, while for A it falls between 0.1 and 1.0 G in the case of monomeric complexes. For the dimeric species, g is much less reliable, its error is likely to be in the order of magnitude of 0.01.
[b] Average of the principal values of the corresponding tensor.
[c] The nitrogen superhyperfine coupling tensor was assumed to be axial; $a_{Nxx} = a_{Nyy}$ are symbolized by $a_{N\perp}$; a_{Nzz} is not given in the Table, since the broad parallel lines did not allow to obtain a reliable value for it.

$[CuH_{-1}\mathbf{AB}_2]$, in contrast to pH-potentiometric findings. This can be explained, on the one hand, by the fact that pH-potentiometry seems to overestimate the mixed–ligand complex formation, compared also to UV–Vis spectral data (see Section 3.1). On the other hand, the decomposition of individual isotropic ESR spectra yields less reliable relative concentrations than the simultaneous analysis of series of spectra (elaborated for binary systems), and can overestimate the contribution of well-resolved spectra – $[CuH_{-1}\mathbf{A}]$ – at the expense of curves with broader lines as for $[CuH_{-1}\mathbf{AB}_2]$.

3.4. ESR spectra in frozen solution at 77 K

The anisotropic spectra are shown in Fig. 6. Their well-resolved character allowed a reliable spectrum-decomposition, offering further information on the coordination modes. It should be noted that for the Cu(II)–H**A** binary system, low temperature promoted also the formation of $[CuH_{-2}\mathbf{A}_2]^{2-}$, resulting a multiply superimposed spectrum at pH 4.67, therefore, we choose the spectrum of a more acidic solution where an unique spectrum decomposition could be carried out. The anisotropic ESR parameters and the relative concentrations for the various species are summarized in Table 5. It can be concluded from the concentration data that freezing induced considerable changes in speciation: (a) it promoted the coordination of **B** to the metal ion both in the Cu(II)–**B** and Cu(II)–H**A**–B systems, and (b) led to the formation of oligomeric species. The former fact is not surprising: Szabó-Plánka et al. have shown [47] that – besides the fact that glass-forming compounds can lower the equilibrium freezing point – a significant undercooling occurs upon fast freezing of the samples, too, so the equilibria "freeze" at considerably lower temperature than the freezing point of dilute aqueous solutions (~273 K). If the formation enthalpies of various species differ from each other significantly, their formation constants alter to different extent upon freezing, in terms of the van't Hoff equation, as it was observed with the Cu(II) – 3-pyridylmethanol system, too.

For the Cu(II)–**B** system, though in liquid solution only $[Cu\mathbf{B}]^{2+}$ and $[Cu\mathbf{B}_2]^{2+}$ could be shown, in frozen solution we could identify also $[Cu\mathbf{B}_3]^{2+}$ and $[Cu\mathbf{B}_4]^{2+}$, moreover, the latter was predominant at 25-fold excess of **B**. Compared to 3-pyridylmethanol, the lower basicity of the donor N of this ligand is manifested in weaker Cu–N bonds, and this leads to higher $g_{\|}$ and lower $A_{\|}$ for the **B** (Table 5) than for the corresponding 3-pyridylmethanol complexes [47].

For the Cu(II)–H**A**–**B** system, the concentration of the mixed–ligand complex is significantly higher in the frozen state than in the same solutions at 298 K (Tables 4 and 5). It should be noted that, compared to $[CuH_{-1}\mathbf{A}]$, the coordination of the two **B** ligands increases ligand field strength in solid phase, too, which is reflected in the significant decrease in g and increase in A for $[CuH_{-1}\mathbf{AB}_2]$ (Table 5).

A further evidence for the favoured ligation of **B** at low temperature is that in frozen solution this ligand, present in high excess, replaces even the chelating "$H_{-1}\mathbf{A}$": at T_B = 25 mM, the spectra of the Cu(II)–**B** and Cu(II)–H**A**–**B** systems are closely similar regarding both their g and A values (Table 5) and superhyperfine patterns (Fig. 6). In the mixed ligand complex $[CuH_{-1}\mathbf{AB}_2]$, a 2 N splitting is expected, however, the resolved superhyperfine structure in the perpendicular region cannot be described by the 2 N model (Fig. 7). We could describe the positions of most superhyperfine lines by the 3 N model, similar to the 4 N model, however, only the latter model could describe satisfactorily also the intensity distribution of the lines (Fig. 6), suggesting the equatorial coordination of four ligands **B**.

In the systems Cu(II)–H**A** and Cu(II)–H**A**–**B**, in frozen solution there is a spectral component with considerable zero-field splitting and very broad lines (Figs. 8 and 9 and Table 5), which suggests oligomerization processes. The nature of these oligomers is difficult to characterize. In the Cu(II)–4-fluorosalicylic acid system, a small amount of $[Cu_2H_{-2}\mathbf{A}_2]$ was shown in liquid solution, where two monomeric units are bridged by the mutual equatorial ligation of the phenolate oxygens to the neighboring metal ions [47]. Probably, the above spectral component (Fig. 8) can be assigned to this species. For the mixed ligand system, the ratio of the spectral

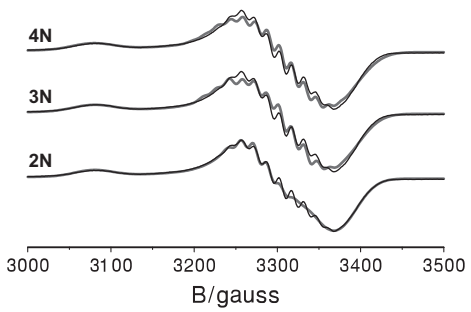

Fig. 7. The experimental curve (black line) taken in 9 v/v% methanol/water at 77 K, at T_{Cu} = 1 mM, T_A = 2 mM and T_B = 25 mM analytical concentrations, pH 4.65, together with the spectra calculated with a 4, 3 or 2 N superhyperfine splitting model (gray line).

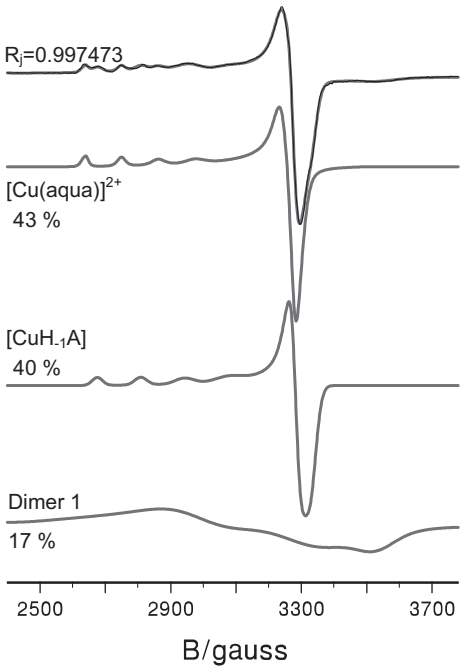

Fig. 8. Top: experimental curve (black line) taken in 9 v/v% methanol/water solution at 77 K, at T_{Cu} = 1 mM and T_A = 2 mM analytical concentrations, pH 4.01, together with the curve calculated as a three-component spectrum (gray line). The component spectra are shown by gray lines (bottom).

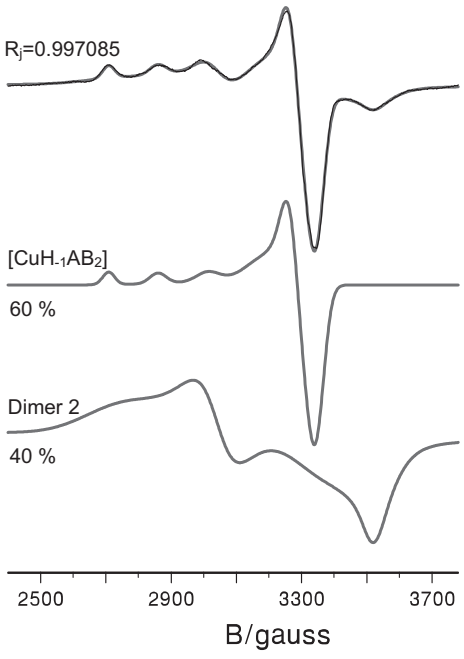

Fig. 9. Top: experimental curve (black line) taken in 9 v/v% methanol/water solution at 77 K, at T_{Cu} = 1 mM, T_A = 2 mM and T_B = 2 mM analytical concentrations, pH 4.67, together with the curve calculated as a two-component spectrum (gray line). The component spectra are shown by gray lines (bottom).

component with zero-field splitting is even higher, so its presence cannot be explained by the dimerization of the minor [CuH_{-1}**A**] alone (if the latter is formed at all under these conditions). Phenolate bridges may connect the monomers of the mixed–ligand complex, too, or carboxylate bridges can be formed between the monomeric units of [Cu$\mathbf{A}_2\mathbf{B}_2$]. These changes would require a considerable rearrangement in the coordination sphere. However, there is not enough experimental evidence for or against the structures of dimeric species.

Finally, it should be noted that the differences between the parameters of the same complex, obtained by the decomposition of different anisotropic spectra, slightly exceed the experimental errors in some cases (Table 5). The most probable reason for this is that, in most cases, the anisotropic spectra were described as the superpositions of two component curves, though different minor complexes might also be present in the solutions in small concentration. A minimum concentration of 10–20% is necessary for the consideration of a species in the decomposition of an anisotropic spectrum. If a complex of lower concentration is included in the model, the uncertainties of all fitted parameters may increase considerably. If, in turn, the corresponding minor species is omitted, the parameters assigned to the major species are slightly modified by the contribution of the neglected species, or, in other words, they are, in fact, average values.

4. Conclusions

The ligand *N*,*N*-diethylnicotinamide is a weak complexing agent, in accordance with the low basicity of its pyridyl nitrogen. At low temperature, its complexation is much more favoured than at 298 K. When both *N*,*N*-diethylnicotinamide and 4-fluorosalicylic acid are present, the formation of mixed–ligand complexes is favoured. In acidic solution, the monodentate ligation of two 4-fluorosalicylate anions and the coordination of two *N*,*N*-diethylnicotinamide molecules occur, and in the crystalline state two water molecules occupy the axial sites of the elongated square-bipyramidal complex, which take part in extensive H-bond network. In moderately acidic solution, where the deprotonated 4-fluorosalicylic acid is chelated to copper(II) by its carboxylate and phenolate oxygens, also the simultaneous ligation of two *N*,*N*-diethylnicotinamide molecules occurs. This mixed–ligand complex is a major species at a moderate, while predominant at a 25-fold excess of *N*,*N*-diethylnicotinamide. At low temperature, four molecules of the latter ligand are coordinated to copper(II), if it is present in high excess, replacing 4-fluorosalicylic acid. Dimers with a considerable zero-field splitting in their spectra are also present in frozen solution; their amount decreases with increasing excess of *N*,*N*-diethylnicotinamide.

Acknowledgments

The work was performed in the framework of Hungarian–Slovak Intergovernmental S&T Cooperation (Project SK-25/2006). Furthermore, the financial support of the Hungarian Scientific Research Fund OTKA (Grants K72781, F67581 and NI61786) and the Slovak Academy of Sciences (Grants VEGA 1/2452/05 and APVT-20-005504) are gratefully acknowledged.

Appendix A. Supplementary data

CCDC 821897 contains the supplementary crystallographic data for this paper. These data can be obtained free of charge via http://www.ccdc.cam.ac.uk/conts/retrieving.html, or from the Cambridge Crystallographic Data Centre, 12 Union Road, Cambridge CB2 1EZ, UK; fax: (+44) 1223-336-033; or e-mail: deposit@ccdc.cam.ac.uk.

References

[1] F.J. Ramos-Lima, A.G. Quiroga, J.M. Perez, C. Navarro-Ranninger, Polyhedron 22 (2003) 3379.
[2] F.J. Ramos-Lima, O. Vrana, A.G. Quiroga, C.N. Navarro-Ranninger, A. Halamikova, H. Rybnickova, L. Hejmalova, V. Brabec, J. Med. Chem. 49 (2006) 2640.
[3] V. Brumas, B. Brumas, G. Berthon, J. Inorg. Biochem. 57 (1995) 191.

[4] S. Gaubert, M. Bouchaut, V. Brumas, G. Berthon, Free Radic. Res. 32 (2000) 451.
[5] V. Brumas, H. Miche, M. Fiallo, J. Inorg. Biochem. 101 (2007) 565.
[6] G.D. Geromichalos, D.T. Trafalis, G.A. Katsoulos, A. Papageorgiou, P. Dalezis, E.B. Triandafillidis, C.C. Hadjikostas, A. Athanassiou, J. Boun. 11 (2006) 469.
[7] A. Martinez, J. Lorenzo, M.J. Prieto, M. Font-Bardia, X. Solans, F.X. Aviles, V. Moreno, Bioorg. Med. Chem. 15 (2007) 969.
[8] K. Svik, M. Stančíková, J. Rovenský, M. Melník, Rheumatologia 9 (1995) 89.
[9] P.M. Wax, J. Toxicol. Clin. Toxicol. 35 (1997) 203.
[10] Z.B. Qian, M.L. Ji, Z.H. Wu, Neural Regen. Res. 5 (2010) 287.
[11] B. Kozlevčar, N. Lah, I. Leban, F. Pohleven, P. Šegedin, Croat. Chim. Acta 73 (2000) 733.
[12] J. Moncol, B. Kalinaková, J. Švorec, M. Kleinová, M. Koman, D. Hudecová, M. Melník, M. Mazúr, M. Valko, Inorg. Chim. Acta 357 (2004) 3211.
[13] A. Arslantas, A.K. Devrim, H. Necefoglu, Int. J. Mol. Sci. 8 (2007) 1225.
[14] P. Segľa, J. Miklovič, D. Mikloš, J. Titiš, R. Herchel, J. Moncol, B. Kalinaková, D. Hudecová, V. Mrazová, T. Lis, M. Melník, Transition Met. Chem. 33 (2008) 967.
[15] P. Segľa, D. Mikloš, J. Jašková, J. Miklovič, B. Kalinaková, D. Hudecová, J. Švorec, T. Lis, M. Melník, J. Coord. Chem. 61 (2008) 3763.
[16] J. Moncol, M. Mudra, P. Lonnecke, M. Hewitt, M. Valko, H. Morris, J. Švorec, M. Melník, M. Mazúr, M. Koman, Inorg. Chim. Acta 360 (2007) 3213.
[17] J. Kavalírová, M. Korabik, P. Stachová, J. Moncol, R. Sillanpää, T. Lis, D. Mikloš, M. Melník, J. Mroziński, D. Valigura, Polyhedron 27 (2008) 1333.
[18] L.Kh. Minacheva, T.S. Khodashova, M.A. Porai-Koshits, A.Yu. Tsivadze, Koord. Khim. 7 (1981) 455.
[19] T. Hökelek, H. Necefoglu, M. Balci, Acta Crystallogr., Sect. C 51 (1995) 2020.
[20] Z. Vasková, J. Moncol, M. Korabik, J. Medvecká, J. Švorec, Z. Padělková, M. Valko, D. Valigura, Polyhedron 30 (2011) 86.
[21] M. Korabik, Z. Repická, L. Martiška, J. Moncol, J. Švorec, Z. Padělková, T. Lis, M. Mazúr, D. Valigura, Z. Anorg. Allg. Chem. 637 (2011) 224.
[22] T. Hökelek, H. Gunduz, H. Necefoglu, Acta Crystallogr., Sect. C 52 (1996) 2470.
[23] M. Koman, M. Melník, T. Glowiak, J. Coord. Chem. 44 (1998) 133.
[24] M. Melník, I. Potočňak, Ľ. Macášková, D. Mikloš, C.E. Holloway, Polyhedron 15 (1996) 2159.
[25] M. Melník, M. Koman, Ľ. Macášková, T. Glowiak, J. Coord. Chem. 44 (1998) 163.
[26] J. Švorec, Š. Lörinc, J. Moncol, M. Melník, M. Koman, Transition Met. Chem. 34 (2009) 703.
[27] J. Moncol, M. Palicova, P. Segľa, M. Koman, M. Melník, M. Valko, T. Glowiak, Polyhedron 31 (2002) 365.
[28] T. Hökelek, K. Budak, H. Necefoglu, Acta Crystallogr., Sect. C 53 (1997) 1049.
[29] Z. Repická, J. Moncol, M. Puchoňová, V. Jorík, D. Mikloš, T. Lis, Z. Padělková, M. Mazúr, D. Valigura, Struct. Chem. 21 (2010) 1093.
[30] J. Moncol, Z. Púčeková, T. Lis, D. Valigura, Acta Crystallogr., Sect. E 62 (2006) m448.
[31] P.A. Mackowiak, Clin. Infect. Dis. 31 (2000) S154.
[32] G. Smith, U.D. Wermuth, J.M. White, Acta Crystallogr., Sect. C 61 (2005) o464.
[33] P.L. Lakatos, L. Lakatos, Pharmacol. Res. 58 (2008) 190.
[34] S.C. Ng, M.A. Kamm, Aliment Pharmacol. Ther. 28 (2008) 815.
[35] L. Gales, M.R. Almeida, G. Arsequell, G. Valencia, M.J. Saraiva, A.M. Damas, Biochim. Biophys. Acta 1784 (2008) 512.
[36] M. da Silva, S.C.M. Menezes, E.I. Ferreira, C.Q.F. Leite, D.N. Sato, C.C. Correia, C.P. Pimenta, K.C.A. Botelho, Chem. Biol. Drug Des. 71 (2008) 167.
[37] V.S. Sumi, R. Kala, R.S. Praveen, T.P. Rao, Int. J. Pharmaceut. 349 (2008) 30.
[38] L. Lazzarato, M. Donnola, B. Rolando, E. Marini, C. Cena, G. Coruzzi, E. Guaita, G. Morini, R. Fruttero, A. Gasco, S. Biondi, E. Ongini, J. Med. Chem. 51 (2008) 1894.
[39] M. Maher, H. Ao, T. Banke, N. Nasser, N.-T. Wu, J.G. Breitenbucher, S.R. Chaplan, A.D. Wickenden, Mol. Pharmacol. 73 (2008) 1225.
[40] Z. Korolkiewicz, E. Hac, E. Gagalo, P. Gorczyca, A. Lodzinska, Agents Actions 26 (1989) 355.
[41] N. Palanisami, G. Prabusankar, R. Murugavel, Inorg. Chem. Commun. 9 (2006) 1002.
[42] C. Lopez-Alarcon, H. Speisky, E. Lissi, Biol. Res. 40 (2007) 155.
[43] M.S. Iqbal, M. Sher, H. Pervez, M. Saeed, Biol. Trace Elem. Res. 124 (2008) 283.
[44] I. Ott, B. Kircher, C.P. Bagowski, D.H.W. Vlecken, E.B. Ott, J. Will, K. Bensdorf, W.S. Sheldrick, R. Gust, Angew. Chem., Int. Ed. 48 (2009) 1160.
[45] T. Szabó-Plánka, B. Gyurcsik, N.V. Nagy, A. Rockenbauer, R. Šípoš, J. Šima, M. Melník, J. Inorg. Biochem. 102 (2008) 101.
[46] R. Šípoš, J. Šima, P. Tarapčik, B. Gyurcsik, Chem. Papers 62 (2008) 496.
[47] R. Šípoš, T. Szabó-Plánka, A. Rockenbauer, N.V. Nagy, J. Šima, M. Melník, I. Nagypál, J. Phys. Chem. A 112 (2008) 10280.
[48] T. Szabó-Plánka, B. Gyurcsik, I. Pálinkó, N.V. Nagy, A. Rockenbauer, R. Šípoš, J. Šima, M. Melník, J. Inorg. Biochem. 105 (2011) 75.
[49] F.J.C. Rosotti, H. Rosotti, The Determination of Stability Constants, McGraw-Hill Book Co., New York, 1962. p. 149.
[50] E. Högfeldt, Stability Constants of Metal–Ion Complexes. Part A. Inorganic Ligands, Pergamon, New York, 1982. p. 32.
[51] L. Zékány, I. Nagypál, G. Peintler, PSEQUAD for Chemical Equilibria, Technical Software Distributors, Baltimore, MD, 1991.
[52] Bruker, APEX2 and SAINT, Bruker AXS Inc., Madison, Wisconsin, USA, 2008.
[53] A. Altomare, M.C. Burla, M. Camalli, G.L. Cascarano, C. Giacovazzo, A. Guagliardi, A.G.G. Moliterni, G. Polidori, R. Spagna, J. Appl. Crystallogr. 32 (1999) 115.
[54] G.M. Sheldrick, Acta Crystallogr., Sect. A 64 (2008) 112.
[55] G.M. Sheldrick, SADABS, University of Göttingen, Germany, 1996.
[56] A.L. Spek, J. Appl. Crystallogr. 36 (2003) 7.
[57] A. Rockenbauer, L. Korecz, Appl. Magn. Reson. 10 (1996) 29.
[58] A.A. Bendryshev, E.B. Pashkova, A.V. Pirogov, O.A. Shpigun, Moscow Univ. Chem. Bull. 65 (2010) 260.
[59] V.B. Korchagin, A.D. Tomashchik, V.I. Vasil'ev, Pharm. Chem. J. 5 (1971) 501.
[60] Beilsteins Handbuch der Organischen Chemie, 4 Aufl., 3 und 4 Ergänzungswerk, Bd. 27, Teil 11, Springer, Berlin, 1984, p. 7980.
[61] T. Sismanoglu, Chin. Chem. Lett. 14 (2003) 1207.
[62] M.R.L. Stratford, M.F. Dennis, P. Hoskin, H. Phillips, R.J. Hodgkiss, A. Rojas, Brit. J. Cancer 74 (1996) 16.
[63] N.I. Jakab, Z. Vasková, J. Moncol, B. Gyurcsik, J. Šima, M. Koman, D. Valigura, Polyhedron 29 (2010) 2262.
[64] J. Gažo, I.B. Bersuker, J. Garaj, M. Kabešová, J. Kohout, H. Langfelderová, M. Melník, M. Serátor, F. Valach, Coord. Chem. Rev. 19 (1976) 253.
[65] J. Bernstein, R.E. Davis, L. Shimoni, N.-L. Chang, Angew. Chem., Int. Ed. Engl. 34 (1995) 1555.
[66] C. Janiak, J. Chem. Soc., Dalton Trans. (2000) 3885.
[67] K. Nakamoto, Infrared and Raman Spectra of Inorganic and Coordination Compounds, Wiley-Interscience, New-York, 1997.
[68] A.B.P. Lever, Inorganic Electronic Spectroscopy, Elsevier, Amsterdam, 1984.